Eur. Phys. J. C (2017) 77:889
https://doi.org/10.1140/epjc/s10052-017-5446-9

THE EUROPEAN PHYSICAL JOURNAL C

Regular Article - Theoretical Physics

The $B-L$ scotogenic models for Dirac neutrino masses

Weijian Wang[1,a], **Ruihong Wang**[2], **Zhi-Long Han**[3], **Jin-Zhong Han**[4]

[1] Department of Physics, North China Electric Power University, Baoding 071003, China
[2] College of Information Science and Technology, Hebei Agricultural University, Baoding, China
[3] School of Physics and Technology, University of Jinan, Jinan 250022, Shandong, China
[4] School of Physics and Telecommunications Engineering, Zhoukou Normal University, Zhoukou 466001, Henan, China

Received: 27 September 2017 / Accepted: 2 December 2017 / Published online: 19 December 2017

Abstract We construct the one-loop and two-loop scotogenic models for Dirac neutrino mass generation in the context of $U(1)_{B-L}$ extensions of standard model. It is indicated that the total number of intermediate fermion singlets is uniquely fixed by the anomaly free condition and the new particles may have exotic $B-L$ charges so that the direct SM Yukawa mass term $\bar{\nu}_L \nu_R \overline{\phi^0}$ and the Majorana mass term $(m_N/2)\overline{\nu_R^C}\nu_R$ are naturally forbidden. After the spontaneous breaking of the $U(1)_{B-L}$ symmetry, the discrete Z_2 or Z_3 symmetry appears as the residual symmetry and gives rise to the stability of intermediate fields as DM candidates. Phenomenological aspects of lepton flavor violation, DM, leptogenesis and LHC signatures are discussed.

1 Introduction

The standard model (SM) needs extensions to incorporate two important missing pieces: the tiny neutrino masses and the cosmological dark matter (DM) candidates. The scotogenic model, proposed by Ma [1], has recently become an attractive and economical scenario to accommodate the above two issues in a unified framework. The main idea is based on the assumption that the DM candidates can serve as intermediate messengers propagating inside the loop diagram in neutrino mass generation. Classical examples are the Ma one-loop model [1] and two-loop model [2]. Some representative variations are found in Refs. [3–31]. In these models, the stability of DM is usually guaranteed by imposing the odd parity under *ad hoc* Z_2 or Z_3 symmetry. The origin of this discrete symmetry is still unknown. An attractive scenario, known as the Krauss–Wilczek mechanism [32], is that the discrete symmetry appears as the residual symmetry which originates from the spontaneous symmetry breaking (SSB) of a continuous gauge symmetry at high scale. The simplest and best-studied gauge extension of SM is that of $U(1)_{B-L}$, which was first realized within the framework of left–right symmetric models [33–36]. In this spirit, several loop-induced Majorana neutrino mass models were constructed based on the gauged $U(1)_{B-L}$ symmetry [37–45]. In this work, exotic $B-L$ charges are assigned to new particles to satisfy the anomaly cancellation condition. By taking an appropriate charge assignment, the residual discrete $Z_2(Z_3)$ symmetry arises after the SSB of the $U(1)_{B-L}$ symmetry. Then the lightest particles with odd $Z_2(Z_3)$ parity cannot decay into SM ingredients, becoming a DM candidate.

On the other hand, the evidence establishing whether neutrinos are Majorana or Dirac fermions is still missing. If neutrinos are Dirac fermions, certain new physics issues beyond the SM should exist to account for the tiny neutrino mass. Several scotogenic models for the Dirac neutrino masses were proposed in Refs. [46–52]. The generic one-loop topographies are discussed in Ref. [53] and, subsequently, specific realizations with $SU(2)_L$ multiplet fields are presented in Ref. [54]. In these models, two *ad hoc* discrete symmetries were introduced. One is responsible for the absence of SM Yukawa couplings $\bar{\nu}_L \nu_R \overline{\phi^0}$ and the other for the stability of intermediate fields as dark matter (DM). The symmetries could be the discrete ones Z_2 [47,53,54], Z_3 [50,55], or Z_4 [56,57].

It is natural to ask if the $B-L$ symmetry also could shed light on Dirac neutrino mass generation and DM phenomena. Recently, several efforts were made at tree level [55,58–60], and a specific one-loop realization was also proposed based on a left–right symmetry scheme [52]. In this brief article, we propose the $U(1)_{B-L}$ extensions of scotogenic Dirac neutrino mass models with intermediate Dirac fermion singlets. We will systematically discuss the

[a] e-mail: wjnwang96@aliyun.com

one- and two-loop realizations for Dirac neutrino masses with typical topographies, respectively. In these models, a singlet scalar σ is responsible for the SSB of the gauged $U(1)_{B-L}$ symmetry as well as the masses of the heavy intermediate Dirac fermions. To get the Dirac type neutrino mass term, we introduce three right-handed components ν_R and assume that they share the $B-L$ charges. The intermediate Dirac fermions are SM singlets but carry $B-L$ quantum numbers. This implies that the anomaly cancellations of $[SU(3)_c]^2 \times U(1)_{B-L}$, $[SU(2)_L]^2 \times U(1)_{B-L}$ and $U(1)_Y \times [U(1)_{B-L}]^2$ are automatically satisfied. Thus we only need to consider the $[U(1)_{B-L}] \times [\text{Gravity}]^2$ and $[U(1)_{B-L}]^3$ anomaly conditions. Then the effective Dirac neutrino mass term $m_D \bar{\nu}_L \nu_R$ is induced by SSB of $U(1)_{B-L}$. As we shall see, the discrete Z_2 or Z_3 symmetry could appear as a remnant symmetry of the gauged $U(1)_{B-L}$ symmetry, naturally leading to DM candidates.

In Sect. 2, we construct the one/two-loop diagrams for Dirac neutrino mass generation and discuss their validity under the $B-L$ anomaly free condition. We consider the phenomenology of the models in Sect. 3. A summary is given in Sect. 4.

2 Model building

2.1 One-loop scotogenic model

Consider first the one-loop scotogenic realization of Dirac neutrino masses. In the $B-L$ extended scotogenic models, the particle content under the $SU(2)_L \times U(1)_Y \times U(1)_{B-L}$ symmetry is listed as follows:

$$\begin{aligned} &L \sim (2, -1/2, -1), \quad \nu_{R1,2,3} \sim (1, 0, Q_{\nu_R}), \\ &F_{L/Ri} \sim (1, 0, Q_{F_{L/R}}), \\ &\Phi \sim (2, 1/2, 0), \quad \eta \sim (2, 1/2, Q_\eta), \\ &\chi \sim (1, 0, Q_\chi), \quad \sigma \sim (1, 0, Q_\sigma), \end{aligned} \tag{1}$$

where several Dirac fermion singlets are added with their chiral components denoted F_{Ri} and F_{Li} ($i = 1 \ldots n$), respectively. In the scalar sector, we further add one doublet scalar η and one singlet scalar χ. After SSB, the vacuum expectation value of Φ and σ can be denoted $\langle\Phi\rangle = v/\sqrt{2}$ and $\langle\sigma\rangle = v_\sigma/\sqrt{2}$. Then the gauge symmetry breaking pattern in this section can be expressed as

$$SU(2)_L \times U(1)_Y \xrightarrow{\langle\Phi\rangle} U(1)_Q, \; U(1)_{B-L} \xrightarrow{\langle\sigma\rangle} Z_2, \tag{2}$$

thus the $B-L$ charge does not contribute to the electric charge. Note that in conventional left–right symmetric models [33–37,52], the gauge symmetry breaking pattern is $SU(2)_L \times SU(2)_R \times U(1)_{B-L} \to SU(2)_L \times U(1)_Y \to U(1)_Q$, hence the $B-L$ charge will contribute to the electric charge.

In the original Z_2 model [46,47], the Z_2 odd parity is assigned to ν_R and intermediate particle fields running in the loop. As a warm-up, we start from the simplest $U(1)_{B-L}$ extension. We call it the A_1 model, with the corresponding Feynman diagrams illustrated as the first diagram in Fig. 1. The relevant interactions for radiative Dirac neutrino mass generation are given as

$$\begin{aligned} \mathcal{L} \supset\; & y_1 \overline{L} F_R i\tau_2 \eta^* + y_2 \overline{\nu_R} F_L \chi + f \overline{F_L} F_R \sigma \\ & + \mu(\Phi^\dagger \eta)\chi^* + \text{h.c.}, \end{aligned} \tag{3}$$

where L is the SM lepton doublet and we omit the summation indices. In terms of gauged $U(1)_{B-L}$ symmetry, one should consider the $[U(1)_{B-L}] \times [\text{Gravity}]^2$ and $[U(1)_{B-L}]^3$ anomaly free conditions

$$\begin{aligned} &-3 - 3Q_{\nu_R} - nQ_{F_R} + nQ_{F_L} = 0, \\ &-3 - 3Q_{\nu_R}^3 - nQ_{F_R}^3 + nQ_{F_L}^3 = 0, \end{aligned} \tag{4}$$

which, using relevant interactions given in Eq. (3), can be solved exactly as

$$n = 3, \qquad Q_{F_R} = -Q_{\nu_R}, \qquad Q_{F_L} = 1. \tag{5}$$

Given the interactions in Eq. (3), the charge assignments for the other particles are listed in the A_1 row in Table 1. Therefore the total number of heavy fermions is fixed by the anomaly free conditions and the $B-L$ charge assignments for all new particles are determined in terms of the free parameter Q_{ν_R}. Let us now discuss precisely what values Q_{ν_R} can take. First, the condition $Q_{\nu_R} \neq -1$ should also be imposed to forbid the SM direct Yukawa coupling term $\bar{\nu}_L \nu_R \overline{\phi^0}$. Second, forbidding Majorana mass terms $(m_R)\overline{\nu_R^C}\nu_R$, $\sigma\overline{\nu_R^C}\nu_R$ and $\sigma^*\overline{\nu_R^C}\nu_R$ requires $Q_{\nu_R} \neq 0, -1/3$ and 1, respectively (note that $Q_\sigma = Q_{\nu_R} + 1$ for A_1 model). Third, to generate a purely loop-induced neutrino mass term, Q_σ and Q_χ $(= Q_{\nu_R} - 1)$ appropriately assigned so that $\sigma^k \chi$ and $(\sigma^*)^k \chi$ $(k = 1, 2, 3)$ terms, which cause the VEV of χ, are forbidden. This further requires $Q_{\nu_R} \neq 0, -1/3, -1/2, -2$ and -3. Similarly, the $(\Phi^\dagger \eta)\sigma^k$ and $(\Phi^\dagger \eta)(\sigma^*)^k$ $(k = 1, 2)$ should also be avoided to generate the VEV of η, leading to $Q_{\nu_R} \neq 0, -1/3, -3$. Once an appropriate Q_{ν_R} is taken, the residual Z_2 symmetry appears in Eq. (3), under which the parity is odd for inert particles $(\eta, \chi, F_{L/R})$ and even for all other particles.

We now consider other possible realizations. In the scalar sector, the interactions relevant to radiative neutrino mass generation are given by

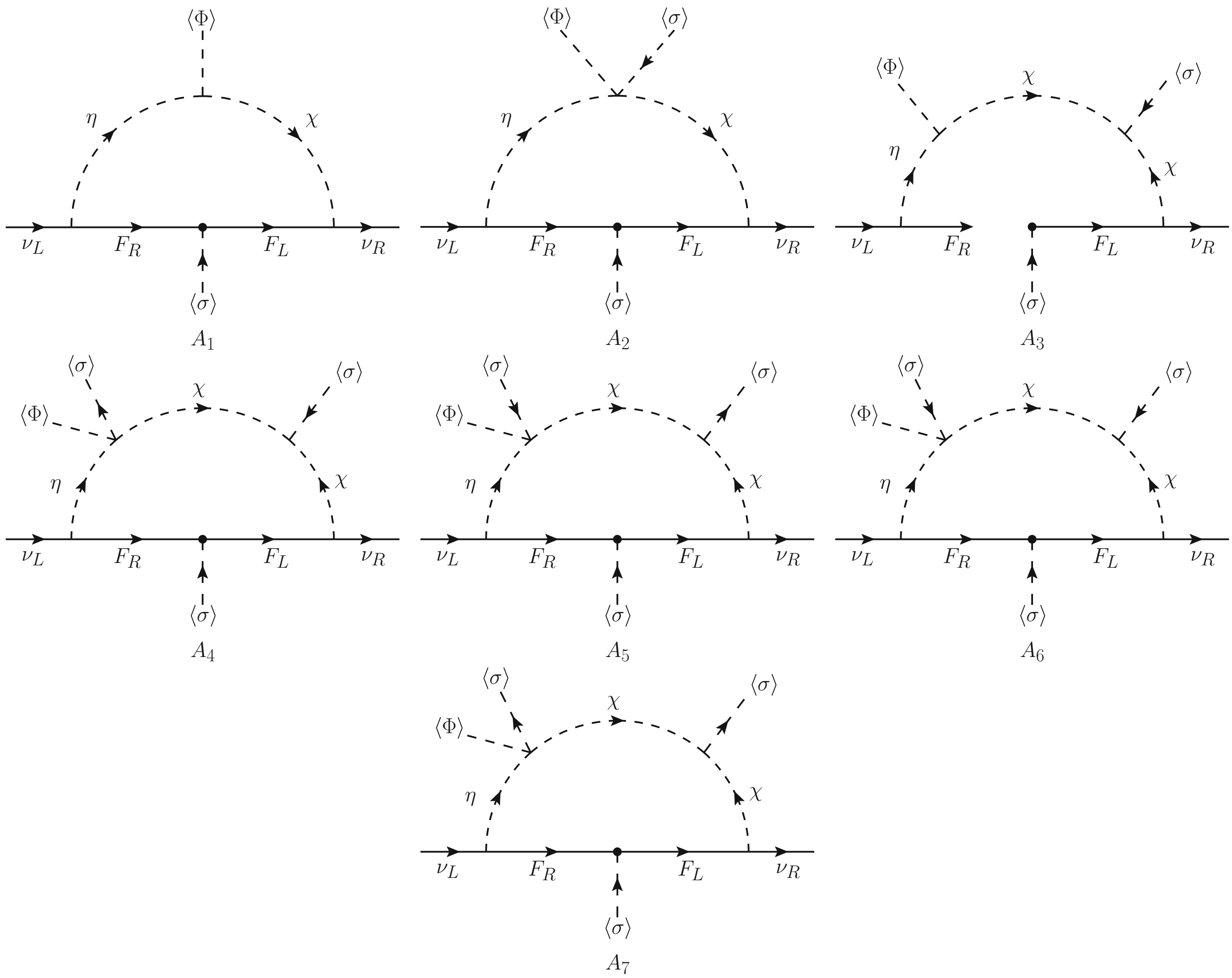

Fig. 1 Possible one-loop topological diagrams that can generate the prototype model given in Ref. [47] after the SSB of the $U(1)_{B-L}$ symmetry

Table 1 $B-L$ charge assignments for new particles in each one-loop models. In $A2$ model, we set $z \equiv (5x^2-6x+5)^{1/2}$. The symbol "×" means that no appropriate charge assignments are available to meet the requirement of anomaly cancellation

Models	n	ν_R	F_R	F_L	η	χ	σ	Scalar interactions
A_1	3	x	$-x$	1	$x-1$	$x-1$	$x+1$	$(\Phi^\dagger\eta)\chi^*$
A_2	6	x	$\frac{\pm z-x-1}{4}$	$\frac{\pm z+x+1}{4}$	$\frac{\mp z+x-3}{4}$	$\frac{\mp z+3x-1}{4}$	$\frac{x+1}{2}$	$(\Phi^\dagger\eta)\chi^*\sigma$
A_3	×	×	×	×	×	×	×	$(\Phi^\dagger\eta)\chi^*,\ \chi^2\sigma$
A_4	3	3	-3	1	2	-2	4	$(\Phi^\dagger\eta)\chi^*\sigma^*,\ \chi^2\sigma$
A_5	3	$\frac{1}{3}$	$-\frac{1}{3}$	1	$-\frac{2}{3}$	$\frac{2}{3}$	$\frac{4}{3}$	$(\Phi^\dagger\eta)\chi^*\sigma,\ \chi^2\sigma^*$
A_6	9	$\frac{23}{13}$	$\frac{5}{13}$	$\frac{17}{13}$	$-\frac{18}{13}$	$-\frac{6}{13}$	$\frac{12}{13}$	$(\Phi^\dagger\eta)\chi^*\sigma,\ \chi^2\sigma$
A_7	×	×	×	×	×	×	×	$(\Phi^\dagger\eta)\chi^*,\ \chi^2\sigma^*$

$$\mathcal{L}_S \supset (\Phi^\dagger\eta)\chi,\quad (\Phi^\dagger\eta)\chi^*,\quad (\Phi^\dagger\eta)\chi\sigma,\quad (\Phi^\dagger\eta)\chi^*\sigma,\quad (\Phi^\dagger\eta)\chi\sigma^*,\quad (\Phi^\dagger\eta)\chi^*\sigma^*,\quad \chi^2\sigma,\quad \chi^2\sigma^*,\quad +\text{h.c.} \tag{6}$$

Taking an appropriate charge assignment, at least one η–χ mixing term given in Eq. (6) should be selected to build the model. All the seven possible topological diagrams (denoted A_1–A_7) are depicted in Fig. 1, where we have already discussed the specific model A_1 above.

Under the gauged $U(1)_{B-L}$ symmetry, the quantum numbers of new particles are required to satisfy the anomaly free conditions. We summarize the $B-L$ quantum number assignments for each diagram in Table 1. We have checked that among the seven models, five of them (A_1, A_2, A_4, A_5 and A_6) are suitable for the gauged $B-L$ extension. For each available model, the total number of intermediate fermions $F_{R/L}$ is uniquely determined by the anomaly free condition of $[U(1)_{B-L}] \times [\text{Gravity}]^2$. The $B-L$ quantum number of the A_1 and A_2 models cannot be uniquely fixed and we choose Q_{ν_R} as the variable. If the χ linear terms are forbidden by the appropriate Q_{ν_R} assignment, the residual Z_2 symmetry arises after the SSB of $U(1)_{B-L}$. Thus the lightest particle with odd Z_2 parity can serve as a DM candidate.

Compared with A_1 and A_2, for models A_4, A_5 and A_6, the $B-L$ quantum numbers for new particles are fixed uniquely. This is due to the fact that the interaction $\chi^2\sigma$ ($\chi^2\sigma^*$) contributes an additional constraint on Q_χ and Q_σ, i.e.,

$$2Q_\chi \pm Q_\sigma = 0. \tag{7}$$

The existence of the $\chi^2\sigma$ ($\chi^2\sigma^*$) term has two-fold meanings: (1) that it automatically forbids the χ linear terms and guarantees the existence of the residual Z_2 symmetry after the SSB of $U(1)_{B-L}$; (2) that it induces a mass splitting $\Delta M = \mid M_{\chi_R} - M_{\chi_I} \mid$ between the real (χ_R) and imaginary part (χ_I) of χ. Provided ΔM is larger than the DM kinetic energy $\text{KE}_\text{D} \sim \mathcal{O}$ (100) KeV, the tree-level DM–nucleon scattering via the $U(1)_{B-L}$ gauge boson Z' and SM Z boson exchange (due to the mixing between η and χ) is kinematically forbidden, thus a χ_R/χ_I dominated DM is expected through the scalar singlet σ or SM Higgs portal.

One recalls that in the prototype scotogenic Dirac model [47] with sizable Yukawa couplings, a relatively small coupling constant of η–χ mixing terms is required to reproduce the scale of the neutrino masses. To rationalize such an unnaturally small coupling, an extra soften broken symmetry is added [47]. We emphasize that the fine tuning can be relaxed in A_4–A_6 models with the help of double suppression from η–χ and χ_R–χ_I mixing interactions. Taking the A_5 model as an example, with scalar interactions $\lambda(\Phi^\dagger\eta)\chi^*\sigma$ and $\mu_\chi\chi^2\sigma^*$, the radiative neutrino mass is evaluated as

$$m_\nu \simeq \frac{\lambda y_1 y_2 f}{16\pi^2}\Big(\frac{\langle\Phi\rangle\langle\sigma\rangle^3}{\Lambda^4}\Big)\mu_\chi, \tag{8}$$

where $\Lambda \sim m_\eta, m_\chi^R, m_\chi^I$ denotes the scale of new physics, usually taken to be $\Lambda \sim \langle\sigma\rangle \sim \mathcal{O}(1)$ TeV. Then, for $\lambda \sim y_1 \sim y_2 \sim f \sim 10^{-2}$ and $\mu_\chi \sim \mathcal{O}$ (10) GeV, the neutrino mass scale (0.1 eV) can be reproduced.

2.2 Two-loop scotogenic models

Now let us discuss the two-loop scotogenic realizations of the Dirac neutrino masses. The simple model with Z_3 discrete symmetry was proposed recently [50], where two classes of Dirac fermion singlets were added. Here we denote the corresponding chiral components by $F_{R,Li}$ ($i = 1, 2\ldots n$) and $S_{R,Lj}$ ($j = 1, 2\ldots m$), respectively. In the scalar sector, we add one scalar doublet η, two scalar singlets χ and ξ. In order to accomplish the $U(1)_{B-L}$ extension, a scalar singlet σ is also added to play a role in the $B-L$ symmetry breaking. The particle content and quantum number assignments under the $SU(2)_L \times U(1)_Y \times U(1)_{B-L}$ gauge symmetry are summarized as follows:

$$\begin{aligned}
&L \sim (2, -1/2, -1), \quad \nu_{R1,2,3} \sim (1, 0, Q_{\nu_R}),\\
&F_{L/Ri} \sim (1, 0, Q_{F_{L/R}}), \quad S_{L/Rj} \sim (1, 0, Q_{S_{L/R}}),\\
&\Phi \sim (2, 1/2, 0), \quad \eta \sim (2, 1/2, Q_\eta), \quad \chi \sim (1, 0, Q_\chi),\\
&\sigma \sim (1, 0, Q_\sigma).
\end{aligned} \tag{9}$$

Similar to the one-loop cases, the two-loop model can be realized through various pathways. As an illustration, we start from a simple $U(1)_{B-L}$ extension (denoted B_1) with topology depicted by the first diagram in Fig. 2. The relevant interactions are

$$\begin{aligned}
\mathcal{L} \supset\ & y_1\overline{L}F_R i\tau_2\eta^* + y_2\overline{\nu_R}S_L\xi + f_1\overline{F_L}F_R\sigma + f_2\overline{S_L}S_R\sigma\\
&+h\overline{S}_R F_L\chi^* + \lambda_1(\Phi^\dagger\eta)\chi^*\sigma + \lambda_2\chi^3\sigma^*\\
&+\mu_3\xi\chi\sigma + \text{h.c.}
\end{aligned} \tag{10}$$

Under the gauged $U(1)_{B-L}$ symmetry, the condition of cancellation for the $[U(1)_{B-L}] \times [\text{Gravity}]^2$ anomaly is given by

$$\begin{aligned}
&-3 - 3Q_{\nu_R} - nQ_{F_R} + n(Q_{F_R} + Q_{\nu_R} + 1) - mQ_{S_R}\\
&\quad+m(Q_{S_R} + Q_{\nu_R} + 1) = 0.
\end{aligned} \tag{11}$$

Notice that $Q_{\nu_R} \neq -1$ is required to forbid the $\overline{\nu}_L\nu_R\overline{\phi^0}$ term. From Eq. (11), one obtains

$$n + m = 3. \tag{12}$$

Clearly, only $(n, m) = (1, 2)$ and $(2, 1)$ patterns are allowed for model B_1. In this scenario, the rank of the effective neutrino mass matrix is two, implying a vanishing neutrino mass eigenvalue. Hence the models with condition $n + m = 3$ are the minimal two-loop realizations allowed phenomenologically. The anomaly free condition of $[U(1)_{B-L}]^3$ is given by

$$\begin{aligned}
&-3 - 3Q_{\nu_R}^3 - nQ_{F_R}^3 + n(Q_{F_R} + Q_{\nu_R} + 1)^3 - mQ_{S_R}^3\\
&\quad+m(Q_{S_R} + Q_{\nu_R} + 1)^3 = 0.
\end{aligned} \tag{13}$$

Taking the interaction terms in Eq. (10) into account and solving Eqs. (12) and (13), we find

$$Q_{\nu_R} = \frac{5n - 17}{3n + 5}. \tag{14}$$

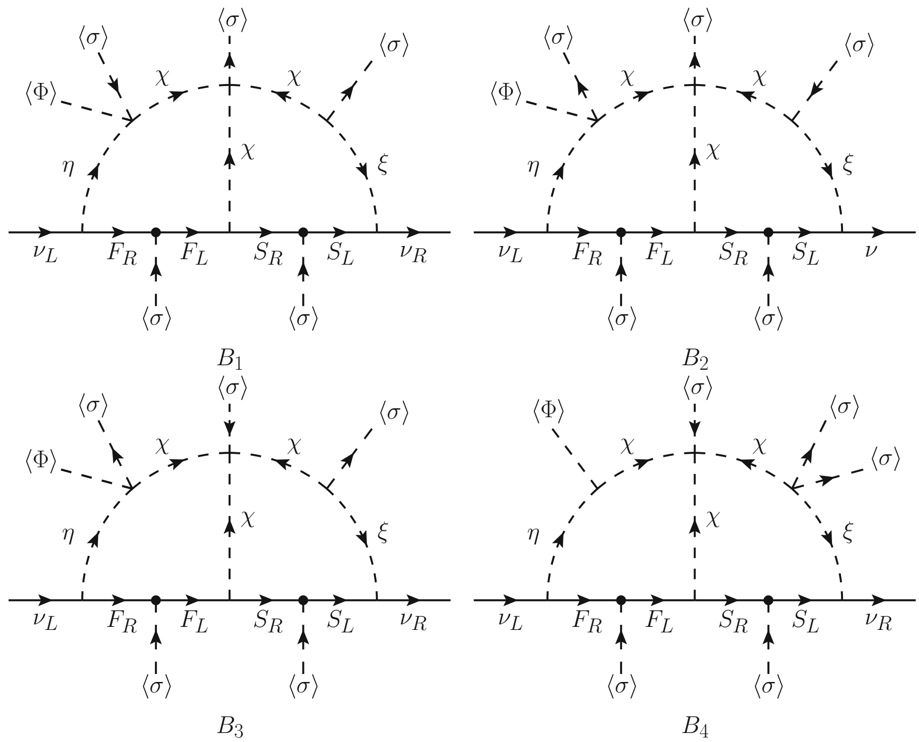

Fig. 2 Available two-loop topological diagrams of Dirac neutrino mass with $n + m = 3$

Table 2 $B - L$ quantum number assignments and relevant scalar interactions for two-loop models with $n + m = 3$

	(n, m)	$\nu_{R1,2,3}$	F_{Ri}	F_{Li}	S_{Ri}	S_{Li}	η	χ	ξ	σ	Scalar interactions
B_1	(1, 2)	$-\frac{1}{11}$	$-\frac{13}{33}$	$\frac{17}{33}$	$\frac{7}{33}$	$\frac{37}{33}$	$-\frac{20}{33}$	$\frac{10}{33}$	$-\frac{40}{33}$	$\frac{10}{11}$	$(\Phi^\dagger\eta)\chi^*\sigma$, $\chi^3\sigma^*$, $\chi\xi\sigma$
	(2, 1)	0	$-\frac{1}{3}$	$\frac{2}{3}$	$\frac{1}{3}$	$\frac{4}{3}$	$-\frac{2}{3}$	$\frac{1}{3}$	$-\frac{4}{3}$	1	$(\Phi^\dagger\eta)\chi^*\sigma$, $\chi^3\sigma^*$, $\chi\xi\sigma$
B_2	(1, 2)	×	×	×	×	×	×	×	×	×	×
	(2, 1)	−11	$\frac{37}{3}$	$\frac{7}{3}$	$\frac{17}{3}$	$-\frac{13}{3}$	$-\frac{40}{3}$	$-\frac{10}{3}$	$-\frac{20}{3}$	−10	$(\Phi^\dagger\eta)\chi^*\sigma^*$, $\chi^3\sigma^*$, $\chi\xi\sigma^*$
B_3	(1, 2)	$-\frac{1}{3}$	$-\frac{13}{9}$	$-\frac{7}{9}$	$-\frac{5}{9}$	$\frac{1}{9}$	$\frac{4}{9}$	$-\frac{2}{9}$	$-\frac{4}{9}$	$\frac{2}{3}$	$(\Phi^\dagger\eta)\chi^*\sigma^*$, $\chi^3\sigma$, $\chi\xi\sigma$
	(2, 1)	−3	$\frac{1}{3}$	$-\frac{5}{3}$	$-\frac{7}{3}$	$-\frac{13}{3}$	$-\frac{4}{3}$	$\frac{2}{3}$	$\frac{4}{3}$	−2	$(\Phi^\dagger\eta)\chi^*\sigma^*$, $\chi^3\sigma$, $\chi\xi\sigma$
B_4	(1, 2)	$-\frac{3}{14}$	$-\frac{31}{42}$	$\frac{1}{21}$	$\frac{13}{42}$	$\frac{23}{21}$	$-\frac{11}{42}$	$-\frac{11}{42}$	$-\frac{55}{42}$	$\frac{11}{14}$	$(\Phi^\dagger\eta)\chi^*$, $\chi^3\sigma$, $\chi\xi\sigma^2$
	(2, 1)	$-\frac{1}{8}$	$-\frac{17}{24}$	$\frac{1}{6}$	$\frac{11}{24}$	$\frac{4}{3}$	$-\frac{7}{24}$	$-\frac{7}{24}$	$-\frac{35}{24}$	$\frac{7}{8}$	$(\Phi^\dagger\eta)\chi^*$, $\chi^3\sigma$, $\chi\xi\sigma^2$

Subsequently, the $B - L$ charges of other particles are obtained, which are shown explicitly in Table 2.

Now we investigate other viable realizations. Without loss of generality, we focus on the minimal models with three intermediate fermions, i.e., $n + m = 3$. To generate a residual Z_3 discrete symmetry, $\chi^3\sigma$ or $\chi^3\sigma^*$ is needed. After the SSB of $U(1)_{B-L}$, χ transforms as $\omega = e^{i2\pi/3}$ under the residual Z_3 symmetry. It is found that only four models are available under the anomaly free condition. The corresponding topological diagrams are shown in Fig. 2. Besides B_1, we denote the rest of the models B_2, B_3 and B_4, respectively. Following the same methodology as in the one-loop case, the $B - L$ charge assignments of new particles for each model are obtained. The main results are listed in Table 2.

Obviously, after $B-L$ breaking, the residual Z_3 symmetry arises with

$$F_{L,Ri} \sim \omega, \qquad S_{L,Ri} \sim \omega, \qquad \eta, \chi \sim \omega, \qquad \xi \sim \omega^2. \tag{15}$$

3 Phenomenology: a case study

In the following, we consider some phenomenological aspects of the gauged $B - L$ scotogenic Dirac models. From Table 1, we can see that besides the $B - L$ charge and some scalar interactions that are different, all the one-loop models have the same interactions as in Eq. (3). Therefore, we can concentrate on the simplest one, i.e., model A_1. As for the two-loop models, the phenomenon will be similar provided the additional ξ and $S_{L,R}$ are heavy enough.

In model A_1, the $B-L$ charges of all the additional particles are determined by the $B-L$ charge of the right-handed neutrino Q_{ν_R}. To ensure a residual Z_2 symmetry after the breaking of $B-L$, we fix $Q_{\nu_R}=1/6$ in the following discussion. The complete gauge invariant scalar potential for model A_1 is

$$\begin{aligned} V = & -\mu_\Phi \Phi^\dagger\Phi + \mu_\eta \eta^\dagger\eta + \mu_\chi \chi^*\chi - \mu_\sigma \sigma^*\sigma \\ & +\lambda_\Phi(\Phi^\dagger\Phi)^2 + \lambda_\eta(\eta^\dagger\eta)^2 + \lambda_\chi(\chi^*\chi)^2 \\ & +\lambda_\sigma(\sigma^*\sigma)^2 + \lambda_{\Phi\eta}(\Phi^\dagger\Phi)(\eta^\dagger\eta) + \lambda_{\Phi\chi}(\Phi^\dagger\Phi)(\chi^*\chi) \\ & +\lambda_{\Phi\sigma}(\Phi^\dagger\Phi)(\sigma^*\sigma) \\ & +\lambda_{\eta\chi}(\eta^\dagger\eta)(\chi^*\chi) + \lambda_{\eta\sigma}(\eta^\dagger\eta)(\sigma^*\sigma) \\ & +\lambda_{\chi\sigma}(\chi^*\chi)(\sigma^*\sigma) + \left[\mu(\Phi^\dagger\eta)\chi^* + \text{h.c.}\right]. \end{aligned} \tag{16}$$

For the Z_2 even scalars, ϕ_R^0 and σ_R mix into physical scalars h and H with mixing angle α. Here, we regard h as the discovered 125 GeV scalar at LHC [61–63]. In order to escape various direct and indirect searches for the scalar H [64,65], a small mixing angle $\sin\alpha = 0.01$ is assumed in this work. Meanwhile, for the Z_2 odd scalars η^0 and χ, they will mix into physical scalars H_2^0 and H_1^0 with mixing angle β. As shown in Refs. [66,67], a small mixing angle, e.g., $\sin\beta \lesssim 0.01$ is preferred in the case of scalar DM H_1^0. In this paper, we take $\sin\beta = 10^{-6}$, mainly aiming to interpret tiny neutrino masses. We also have one pair of Z_2 odd charged scalar $H_2^\pm (=\eta^\pm)$.

Given the interactions in Eq. (3), the one-loop induced neutrino mass for model A_1 is

$$\begin{aligned} m_\nu^{ij} = & \frac{\sin 2\beta}{32\pi^2}\sum_k y_1^{ik} y_2^{jk*} M_{Fk}\left[\frac{M^2_{H_2^0}}{M^2_{H_2^0}-M^2_{Fk}}\ln\left(\frac{M^2_{H_2^0}}{M^2_{Fk}}\right)\right. \\ & \left. -\frac{M^2_{H_1^0}}{M^2_{H_1^0}-M^2_{Fk}}\ln\left(\frac{M^2_{H_1^0}}{M^2_{Fk}}\right)\right]. \end{aligned} \tag{17}$$

To give some concrete prediction, we present one promising benchmark point (BP) for model A_1,

$$\begin{aligned} & \sin\beta = 10^{-6}, |y_{1,2}^{i1}| = 10^{-6}, |y_{1,2}^{i2,i3}| = 0.007, \\ & M_{H_1^0} = 45\text{ GeV}, M_H = 100\text{ GeV}, M_{H_2^\pm, H_2^0} = 600\text{ GeV}, \\ & M_{F1} = M_{F2,F3}/2 = 5\text{ TeV}, M_{Z'} = 4\text{ TeV}, g_{BL} = 0.1, \end{aligned} \tag{18}$$

which could realize $m_\nu \sim 0.1$ eV. For simplicity, we denote $|y_{1,2}^{i2,i3}| = y$ in the following.

Firstly, the existence of the Yukawa interaction $\overline{L} F_R i\tau_2\eta^*$ will induce various lepton flavor violation (LFV) processes. Detailed studies on LFV processes in scotogenic models can be found in Ref. [68]. Here, we take the current most stringent one, i.e., the MEG experiment on the radiative decay $\mu\to e\gamma$ with BR $(\mu\to e\gamma) < 4.2\times10^{-13}$ [69,70], for illustration. The future limit might be down to 6×10^{-14} [71]. In the scotogenic Dirac models, the analytical expression for the branching ratio of $\mu\to e\gamma$ is calculated to be [68]

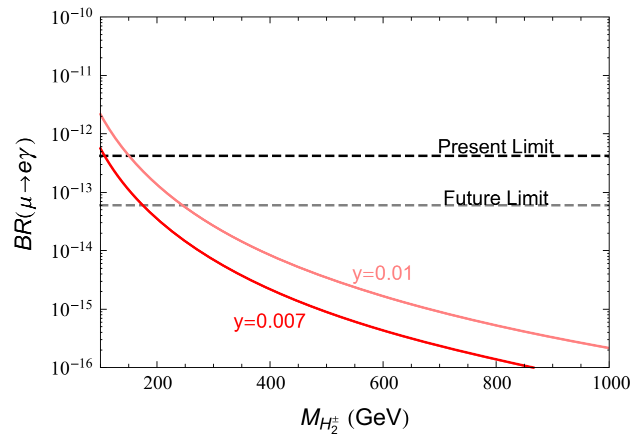

Fig. 3 BR $(\mu\to e\gamma)$ as a function of $M_{H_2^\pm}$

$$\text{BR}(\mu\to e\gamma) = \frac{3\alpha}{64\pi G_F^2}\left|\sum_i \frac{(y_1)_{\mu i}(y_1)^*_{ei}}{M^2_{H_2^+}} F\left(\frac{M^2_{F_i}}{M^2_{H_2^+}}\right)\right|^2, \tag{19}$$

where the loop function $F(x)$ is

$$F(x) = \frac{1-6x+3x^2+2x^3-6x^2\ln x}{6(1-x)^4}. \tag{20}$$

In Fig. 3, we show the BR $(\mu\to e\gamma)$ as a function of $M_{H_2^\pm}$ for $y = 0.01, 0.007$. Our BP in Eq. (18) predicts BR $(\mu\to e\gamma)\approx 4\times10^{-16}$, which is far below current and even future experimental limits.

Secondly, we briefly discuss the phenomenology of dark matter (DM). In this paper, we mainly consider the scalar DM candidate, since for the fermion singlet, $M_F = f\langle\sigma\rangle$ is naturally around the TeV-scale and it is more interesting to realize successful leptogenesis. We emphasize that the $(\Phi^\dagger\eta)^2$ term is not allowed in $U(1)_{B-L}$ extensions to generate a mass splitting between η_R^0 and η_I^0, rendering the η dominated component H_2^0 unsuitable as a DM candidate to escape the direct detection bound. Therefore, we concentrate on the χ dominated component H_1^0 as the DM candidate.

With heavy F and relatively small Yukawa couplings, i.e., $|y_2|\lesssim 0.01$, the contribution of F to H_1^0 annihilation is negligible. To generate the correct relic density, the possible annihilation channels are: (1) SM Higgs h portal; (2) scalar singlet H portal; (3) gauge boson Z' portal. For case (1), the extensive research implies that $M_{H_1^0}\lesssim M_h/2$ is the only allowed region under tight constraints from relic density and direct detection [72,73]. For case (2), $M_{H_1^0}\sim M_H/2$ is needed, and the electroweak scale H_1^0 DM is allowed [74]. Notably,

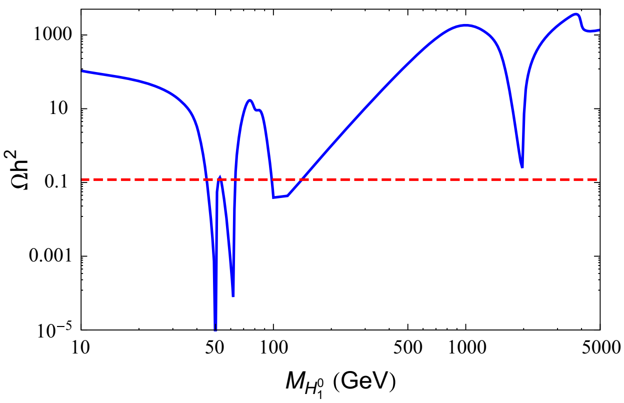

Fig. 4 Ωh^2 as a function of $M_{H_1^0}$. Here, we also fix $\lambda_{\Phi\chi} = \lambda_{\chi\sigma} = 0.001$

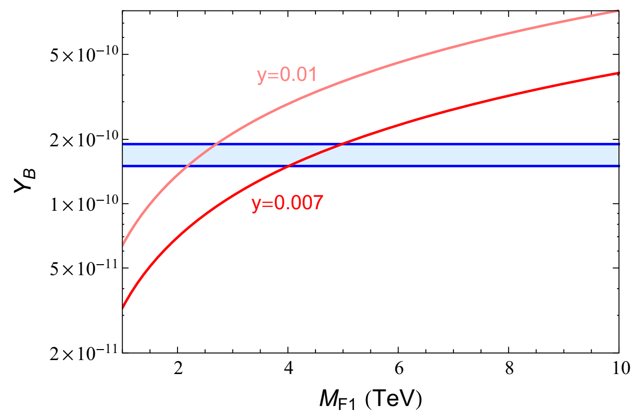

Fig. 5 Y_B as a function of M_{F_1}. The blue bound corresponds to 2σ range of Planck result

when $M_H \sim 100$ GeV, thus $M_{H_1^0} \sim 50$ GeV, the observed excess in gamma-ray flux by Fermi-LAT can be interpreted [75,76]. For case (3), one requires $M_{H_1^0} \sim M_{Z'}/2$, and $M_{H_1^0}$ is usually around the TeV-scale [77]. In Fig. 4, we show the relic density Ωh^2 as a function of $M_{H_1^0}$. The Higgs h/H portal could easily acquire the correct relic density, while the Z' portal could not, due to too small g_{BL}. Note that the process $H_1^0 H_1^{0*} \to HH$ could also realize the correct relic density provided $M_{H_1^0} \sim M_H$.

Thirdly, we consider Dirac leptogenesis. It is well known that the leptogenesis can be accomplished in Dirac neutrino models [78,79]. In model A_1, the heavy fermion singlet F can decay into $L\eta$ and $\nu_R\chi$ to generate lepton asymmetry in the left-handed ϵ_L and right-handed sector ϵ_R. Due to the fact that the sphaleron processes do not have a direct effect on the right-handed fields, the lepton asymmetry in the left-handed sector can be converted into a net baryon asymmetry via sphaleron processes, as long as the one-loop induced effective Dirac Yukawa couplings are small enough to prevent the lepton asymmetry from equilibration before the electroweak phase transition [80].

Under the assumption $y_1 = y_2$, the final lepton asymmetry is calculated as [46]

$$\epsilon_{F_1} \simeq -\frac{1}{8\pi}\frac{1}{(y_1^\dagger y_1)_{11}}\sum_{j\neq 1}\frac{M_{F_1}}{M_{F_j}}\mathrm{Im}\left[(y_1^\dagger y_1)^2_{1j}\right]. \tag{21}$$

Define the parameter $K = \Gamma_{F_1}/H(T = M_{F_1})$, where Γ_{F1} is the tree-level decay width of F_1 and $H(T) = \sqrt{8\pi^3 g_*/90}\,T^2/M_{\rm Pl}$ wit $g_* \simeq 114$ and $M_{\rm Pl} = 1.2 \times 10^{19}$ GeV. As in our case $K \gtrsim 1$, the final baryon asymmetry is estimated as [80]

$$Y_B = -\frac{28}{79}Y_{L_{\nu_R}} \approx -\frac{28}{79}\frac{\epsilon_{F_1}}{g_*}\frac{0.12}{K^{1.1}}. \tag{22}$$

In Fig. 5, we depict Y_B as a function of M_{F_1}. It is clear that the BP in Eq. (18) could predict the correct value of Y_B, as well as satisfy the out of equilibration condition

$$\frac{|y_1|^2|y_2|^2}{M_{F_1}} \lesssim \frac{1}{M_{\rm Pl}}\sqrt{\frac{8\pi^3 g_*}{90}}. \tag{23}$$

Then we turn to the collider phenomenology. The DM candidate H_1^0 will contribute to invisible Higgs decay. The corresponding decay width for $h \to H_1^0 H_1^{0*}$ is calculated to be

$$\Gamma(h \to H_1^0 H_1^{0*}) = \frac{g^2_{hH_1^0H_1^{0*}}}{16\pi M_h}\sqrt{1-4\frac{M^2_{H_1^0}}{M_h^2}}, \tag{24}$$

where $g_{hH_1^0H_1^{0*}} = \lambda_{\Phi\chi} v \cos\alpha + \lambda_{\chi\sigma} v_\sigma \sin\alpha$ is the effective trilinear $hH_1^0H_1^{0*}$ coupling and $v = 246$ GeV, $v_\sigma = M_{Z'}/(g_{BL}Q_\sigma)$. So the invisible branching ratio is $\mathrm{BR_{inv}} = \Gamma_{\rm inv}/(\Gamma_{\rm inv}+\Gamma_{\rm SM})$ with $\Gamma_{\rm SM} = 4.07$ MeV at $M_h = 125$ GeV [81]. Our BP in Eq. (18) with $\lambda_{\Phi\chi} = \lambda_{\chi\sigma} = 0.001$ predicts $\mathrm{BR_{inv}} \sim 0.01$, which can escape the most stringent bound, which comes from fitting to visible Higgs decays, i.e., $\mathrm{BR_{inv}} < 0.23$ [82]. As for the light scalar H, the dominant visible decay is $H \to b\bar{b}$ and the invisible decay is $H \to H_1^0 H_1^{0*}$. The possible promising signatures are $e^+e^- \to ZH$ at future lepton colliders [83]. Meanwhile, due to the doublet nature of $H_2^\pm$ and H_2^0, they can be pair produced at LHC via Drell–Yan processes as $pp \to H_2^+H^-$, $H_2^\pm H_2^{0(*)}$, $H_2^0 H_2^{0*}$. In the case of light H_1^0 DM, the most promising signature is

$$pp \to H_2^\pm H_2^{0(*)} \to W^\pm Z + H_1^0 H_1^{0*}, \tag{25}$$

then leptonic decays of W and Z will induce the trilepton signature $2l^\pm l^- + \not{E}_T$. The direct searches for such a trilepton

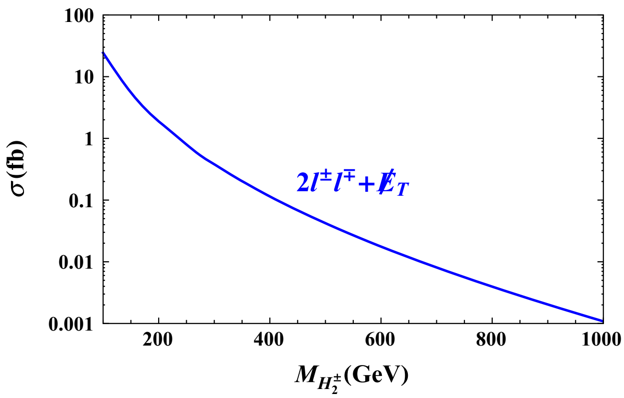

Fig. 6 Trilepton signature $2\ell^\pm\ell^\mp$ as a function of $M_{H_2^\pm}$ at 13 TeV LHC

signature at LHC have excluded $M_{H_2^\pm, H_2^0} \lesssim 350$ GeV when $M_{H_1^0} \sim 50$ GeV [84,85].

In Fig. 6, we show the cross section of trilepton signature at 13 TeV LHC. The cross section of our BP in Eq. (18) is about 0.02 fb.

The gauged $U(1)_{B-L}$ symmetry predicts Z' boson with mass $M_{Z'} = Q_\sigma g_{BL} v_\sigma$. Since the σ scalar is SM singlet and Φ does not transform under $U(1)_{B-L}$, there is no mixing between the Z and the Z' boson. The LEP II data requires that [86]

$$\frac{M_{Z'}}{g_{BL}} = Q_\sigma v_\sigma \gtrsim 6 \sim 7\ \text{TeV}. \tag{26}$$

The direct searches for Z' with SM-like gauge coupling in the dilepton final states have excluded $M_{Z'} \lesssim 4$ TeV [87]. Recasting of these searches in gauged $U(1)_{B-L}$ has been performed in Refs. [77,88], where the exclusion region in the $M_{Z'}$–g_{BL} graphics is obtained. In this paper, we consider $M_{Z'} = 4$ TeV and $g_{BL} = 0.1$ to respect these bounds. In the limit that masses of SM fermions $f(f \equiv q, l, \nu_{L,R})$ are small compared with the Z' mass, the decay width of Z' into a fermion pair, $f\overline{f}$, is given by

$$\Gamma(Z' \to f\overline{f}) = \frac{g_{BL}^2 M_{Z'}}{24\pi} C_f (Q_{fL}^2 + Q_{fR}^2) \tag{27}$$

where $C_{l,\nu} = 1$, $C_q = 3$. Then the branching ratios of Z' decay into each final states take the values

$$\begin{aligned}&\text{BR}(Z' \to q\overline{q}) : \text{BR}(Z' \to l^- l^+) : \text{BR}(Z' \to \nu\overline{\nu}) \\ &\quad = 4 : 6 : 3(1 + Q_{\nu_R}^2),\end{aligned} \tag{28}$$

where $l = e, \mu$. Thus, the $B-L$ nature of Z' can be confirmed when $\text{BR}(Z' \to b\bar{b})/\text{BR}(Z' \to \mu^+\mu^-) = 1/3$ is measured [40]. In addition, the decay width of Z' into the scalar pair SS^* is given by

Table 3 Decay branching ratio of Z'

$q\bar{q}$	$\ell\bar{\ell}$	$\nu\bar{\nu}$	HH	$H_1^0 H_1^{0*}$	$H_2^0 H_2^{0*}$	$H_2^+ H_2^-$
0.27	0.41	0.21	0.05	0.02	0.02	0.02

$$\Gamma(Z' \to SS^*) = \frac{g_{BL}^2}{48\pi} M_{Z'} Q_S^2 \tag{29}$$

in the limit $M_S \ll M_{Z'}$ as well. In the case of H_1^0 DM with the special mass spectrum $M_{H_1^0} < M_H < M_{\eta^\pm, H_2^0} < M_{Z'} < M_F$, as we discussed above, the dominant invisible decays of Z' are $Z' \to \nu\overline{\nu}$ and $Z' \to H_1^0 H_1^{0*}$, and the subdominant contributions are coming from cascade decays as $Z' \to HH$ with $H \to H_1^0 H_1^{0*}$ and $Z' \to H_2^0 H_2^{0*}$ with $H_2^0 \to Z(\to \nu\overline{\nu})H_1^0$. In Table 3, we show the branching ratio of Z' predicted by our BP. Due to the different values of the $B-L$ charges for the new particles in all the possible models present in Tables 1 and 2, they can be distinguished by precise measurement of the invisible decays of Z'.

4 Conclusion

In conclusion, we propose the $U(1)_{B-L}$ extensions of the scotogenic models with intermediate fermion singlets added. The Dirac nature of neutrinos is protected by $B-L$ symmetry, while the DM stability is guaranteed by the residual symmetry of $B-L$ SSB. Under gauged $U(1)_{B-L}$, the values of the $B-L$ quantum numbers for new particles are assigned to satisfy the anomaly free condition. We first present the topological diagrams of one-loop Z_2 realizations and subsequently check their validity under the anomaly free condition. Among the seven one-loop realizations, five of them are available (A_1, A_2, A_4, A_5 and A_6). It is found that the total number of intermediate fermion singlets is uniquely fixed by the anomaly free condition. Especially, the $B-L$ charge assignments for the A_4, A_5 and A_6 models can also be uniquely fixed due to the mass splitting terms in the scalar sector. We emphasize the implications of such terms on alleviating the fine tuning in the model and also permitting intermediate scalar singlet as a DM candidate. Then we study the two-loop Z_3 realizations where n $F_{R/L}$ and m $S_{R/L}$ fermion singlets are added. Doing the same in the one-loop model, we found $n+m$ and $B-L$ charge assignments of all new particles to be uniquely determined by the anomaly free condition. Without loss of generality, we consider the minimal realizations with $n+m=3$ and found four viable models (denoted B_1, B_2, B_3 and B_4).

By considering the phenomenology on lepton flavor violation, dark matter, leptogenesis and LHC signatures, we consider the benchmark point in Eq. (18). In addition to generating a tiny neutrino mass via scalar DM mediator, this BP can also interpret the gamma-ray excess from the galactic center and realize successful leptogenesis. As for collider signatures, the scalar DM H_1^0 will contribute to invisible Higgs decay as $h \to H_1^0 H_1^{0*}$. The scalar singlet H might be testable via $e^+e^- \to ZH$ with $H \to b\bar{b}/H_1^0 H_1^{0*}$ at lepton colliders. Meanwhile, the promising signature at LHC is the trilepton signature as $pp \to H_2^\pm H_2^{0(*)} \to W^\pm Z + H_1^0 H_1^{0*}$ with leptonic decays of W/Z. The new $B-L$ gauge boson is expected discovered via the dilepton signature $pp \to Z' \to l^+l^-$ at LHC [89]. In principle, the constructed models in Tables 1 and 2 can be distinguished by a precise measurement of the invisible decays of Z'.

Acknowledgements The work of Weijian Wang is supported by National Natural Science Foundation of China under Grant numbers 11505062, Special Fund of Theoretical Physics under Grant numbers 11447117 and Fundamental Research Funds for the Central Universities under Grant numbers 2016MS133. The work of Zhi-Long Han is supported in part by the Grants no. NSFC-11575089.

References

1. E. Ma, Phys. Rev. D **73**, 077301 (2006). arXiv:hep-ph/0601225
2. E. Ma, Phys. Lett. B **662**, 49 (2008). arXiv:0708.3371 [hep-ph]
3. E. Ma, D. Suematsu, Mod. Phys. Lett. A **24**, 583 (2009). arXiv:0809.0942 [hep-ph]
4. E. Ma, I. Picek, B. Radovcic, Phys. Lett. B **726**, 744 (2013). arXiv:1308.5313 [hep-ph]
5. S.S.C. Law, K.L. McDonald, JHEP **1309**, 092 (2013). arXiv:1305.6467 [hep-ph]
6. L.M. Krauss, S. Nasri, M. Trodden, Phys. Rev. D **67**, 085002 (2003)
7. M. Aoki, S. Kanemura, O. Seto, Phys. Rev. Lett. **102**, 051805 (2009). arXiv:0807.0361 [hep-ph]
8. M. Gustafsson, J.M. No, M.A. Rivera, Phys. Rev. Lett **110**, 211802 (2013)
9. A. Ahriche, K.L. McDonald, S. Nasri, JHEP **1410**, 167 (2014). arXiv:1404.5917 [hep-ph]
10. S. Baek, H. Okada, K. Yagyu, JHEP **1504**, 049 (2015). arXiv:1501.01530 [hep-ph]
11. E. Ma, Phys. Rev. Lett. **115**(1), 011801 (2015). arXiv:1502.02200 [hep-ph]
12. S. Fraser, C. Kownacki, E. Ma, O. Popov, Phys. Rev. D **93**(1), 013021 (2016). arXiv:1511.06375 [hep-ph]
13. R. Ding, Z.L. Han, Y. Liao, W.P. Xie, JHEP **1605**, 030 (2016). arXiv:1601.06355 [hep-ph]
14. A. Ahriche, K.L. McDonald, S. Nasri, JHEP **1606**, 182 (2016). arXiv:1604.05569 [hep-ph]
15. A. Ahriche, A. Manning, K.L. McDonald, S. Nasri, Phys. Rev. D **94**(5), 053005 (2016). arXiv:1604.05995 [hep-ph]
16. K. Cheung, T. Nomura H. Okada, Phys. Rev. D **95**(1), 015026 (2017). https://doi.org/10.1103/PhysRevD.95.015026. arXiv:1610.04986 [hep-ph]
17. T. Nomura, H. Okada, Y. Orikasa, Phys. Rev. D **94**(11), 115018 (2016). arXiv:1610.04729 [hep-ph]
18. T. Nomura, H. Okada, Y. Orikasa, Phys. Rev. D **94**(11), 115018 (2016). arXiv:1610.04729 [hep-ph]
19. S.Y. Guo, Z.L. Han, Y. Liao, Phys. Rev. D **94**(11), 115014 (2016). arXiv:1609.01018 [hep-ph]
20. W.B. Lu, P.H. Gu, Nucl. Phys. B **924**, 279 (2017). https://doi.org/10.1016/j.nuclphysb.2017.09.005. arXiv:1611.02106 [hep-ph]
21. Z. Liu, P.H. Gu, Nucl. Phys. B **915**, 206 (2017). arXiv:1611.02094 [hep-ph]
22. P.H. Gu, JHEP **1704**, 159 (2017). https://doi.org/10.1007/JHEP04(2017)159. arXiv:1611.03256 [hep-ph]
23. P. Ko, T. Nomura, H. Okada, Phys. Lett. B **772**, 547 (2017). https://doi.org/10.1016/j.physletb.2017.07.021. arXiv:1701.05788 [hep-ph]
24. K. Cheung, T. Nomura, H. Okada, Phys. Lett. B **768**, 359 (2017). https://doi.org/10.1016/j.physletb.2017.03.021. arXiv:1701.01080 [hep-ph]
25. S. Lee, T. Nomura, H. Okada. arXiv:1702.03733 [hep-ph]
26. S. Baek, H. Okada, Y. Orikasa. arXiv:1703.00685 [hep-ph]
27. A.E. Carcamo Hernandez, S. Kovalenko, I. Schmidt, JHEP **1702**, 125 (2017). arXiv:1611.09797 [hep-ph]
28. D. Aristizabal Sierra, C. Simoes, D. Wegman, JHEP **1607**, 124 (2016). arXiv:1605.08267 [hep-ph]
29. C. Simoes, D. Wegman, JHEP **1704**, 148 (2017). https://doi.org/10.1007/JHEP04(2017)148. arXiv:1702.04759 [hep-ph]
30. T. Nomura, H. Okada, Phys. Rev. D **96**(1), 015016 (2017). https://doi.org/10.1103/PhysRevD.96.015016. arXiv:1704.03382 [hep-ph]
31. T. Nomura, H. Okada, Phys. Lett. B **774**, 575 (2017). https://doi.org/10.1016/j.physletb.2017.10.033. arXiv:1704.08581 [hep-ph]
32. K.M. Krauss, F. Wilczek, Phys. Rev. Lett. **62**, 1221 (1989)
33. J.C. Pati, A. Salam, Phys. Rev. D **10**, 275 (1974). Erratum: [Phys. Rev. D **11**, 703 (1975)]
34. R.N. Mohapatra, J.C. Pati, Phys. Rev. D **11**, 2558 (1975)
35. G. Senjanovic, R.N. Mohapatra, Phys. Rev. D **12**, 1502 (1975)
36. R.N. Mohapatra, R.E. Marshak, Phys. Rev. Lett. **44**, 1316 (1980). Erratum: [Phys. Rev. Lett. **44**, 1643 (1980)]
37. A. Adulpravitchai, M. Lindner, A. Merle, R.N. Mohapatra, Phys. Lett. B **680**, 476 (2009). arXiv:0908.0470 [hep-ph]
38. S. Kanemura, O. Seto, T. Shimomura, Phys. Rev. D **84**, 016004 (2011). arXiv:1101.5713 [hep-ph]
39. W.F. Chang, C.F. Wong, Phys. Rev. D **85**, 013018 (2012). arXiv:1104.3934 [hep-ph]
40. S. Kanemura, T. Nabeshima, H. Sugiyama, Phys. Rev. D **85**, 033004 (2012). arXiv:1111.0599 [hep-ph]
41. S. Kanemura, T. Matsui, H. Sugiyama, Phys. Rev. D **90**, 013001 (2014). arXiv:1405.1935 [hep-ph]
42. W. Wang, Z.L. Han, Phys. Rev. D **92**, 095001 (2015). arXiv:1508.00706 [hep-ph]
43. E. Ma, N. Pollard, O. Popov, M. Zakeri, Mod. Phys. Lett. A **31**(27), 1650163 (2016). arXiv:1605.00991 [hep-ph]
44. S.Y. Ho, T. Toma, K. Tsumura, Phys. Rev. D **94**(3), 033007 (2016). arXiv:1604.07894 [hep-ph]
45. O. Seto, T. Shimomura, Phys. Rev. D **95**(9), 095032 (2017). https://doi.org/10.1103/PhysRevD.95.095032. arXiv:1610.08112 [hep-ph]
46. P.H. Gu, U. Sarkar, Phys. Rev. D **77**, 105031 (2008). arXiv:0712.2933 [hep-ph]
47. Y. Farzan, E. Ma, Phys. Rev. D **86**, 033007 (2012). arXiv:1204.4890 [hep-ph]
48. H. Okada. arXiv:1404.0280 [hep-ph]
49. S. Kanemura, K. Sakurai, H. Sugiyama, Phys. Lett. B **758**, 465 (2016). arXiv:1603.08679 [hep-ph]

50. C. Bonilla, E. Ma, E. Peinado, J.W.F. Valle, Phys. Lett. B **762**, 214 (2016). https://doi.org/10.1016/j.physletb.2016.09.027. arXiv:1607.03931 [hep-ph]
51. D. Borah, A. Dasgupta, JCAP **1612**(12), 034 (2016). arXiv:1608.03872 [hep-ph]
52. D. Borah, A. Dasgupta. arXiv:1702.02877 [hep-ph]
53. E. Ma, O. Popov, Phys. Lett. B **764**, 142 (2017). arXiv:1609.02538 [hep-ph]
54. W. Wang, Z.L. Han. arXiv:1611.03240 [hep-ph]
55. E. Ma, N. Pollard, R. Srivastava, M. Zakeri, Phys. Lett. B **750**, 135 (2015). arXiv:1507.03943 [hep-ph]
56. J. Heeck, W. Rodejohann, Europhys. Lett. **103**, 32001 (2013). arXiv:1306.0580 [hep-ph]
57. J. Heeck, Phys. Rev. D **88**, 076004 (2013). arXiv:1307.2241 [hep-ph]
58. E. Ma, R. Srivastava, Phys. Lett. B **741**, 217 (2015). arXiv:1411.5042 [hep-ph]
59. E. Ma, R. Srivastava, Mod. Phys. Lett. A **30**(26), 1530020 (2015). arXiv:1504.00111 [hep-ph]
60. S. Centelles Chulia, E. Ma, R. Srivastava, J.W.F. Valle, Phys. Lett. B **767**, 209 (2017). arXiv:1606.04543 [hep-ph]
61. G. Aad et al. [ATLAS Collaboration], Phys. Lett. B **716**, 1 (2012). arXiv:1207.7214 [hep-ex]
62. S. Chatrchyan et al. [CMS Collaboration], Phys. Lett. B **716**, 30 (2012). arXiv:1207.7235 [hep-ex]
63. G. Aad et al. [ATLAS and CMS Collaborations], Phys. Rev. Lett. **114**, 191803 (2015). arXiv:1503.07589 [hep-ex]
64. T. Robens, T. Stefaniak, Eur. Phys. J. C **75**, 104 (2015). arXiv:1501.02234 [hep-ph]
65. T. Robens, T. Stefaniak, Eur. Phys. J. C **76**(5), 268 (2016). arXiv:1601.07880 [hep-ph]
66. T. Cohen, J. Kearney, A. Pierce, D. Tucker-Smith, Phys. Rev. D **85**, 075003 (2012). arXiv:1109.2604 [hep-ph]
67. M. Kakizaki, A. Santa, O. Seto, Int. J. Mod. Phys. A **32**, 1750038 (2017). arXiv:1609.06555 [hep-ph]
68. T. Toma, A. Vicente, JHEP **1401**, 160 (2014). arXiv:1312.2840, arXiv:1312.2840 [hep-ph]
69. J. Adam et al. [MEG Collaboration], Phys. Rev. Lett. **110**, 201801 (2013). arXiv:1303.0754 [hep-ex]
70. A.M. Baldini et al. [MEG Collaboration], Eur. Phys. J. C **76**(8), 434 (2016). arXiv:1605.05081 [hep-ex]
71. A.M. Baldini et al. arXiv:1301.7225 [physics.ins-det]
72. J.M. Cline, K. Kainulainen, P. Scott, C. Weniger, Phys. Rev. D **88**, 055025 (2013). Erratum: [Phys. Rev. D **92**(3), 039906 (2015)]. arXiv:1306.4710 [hep-ph]
73. X.G. He, J. Tandean, JHEP **1612**, 074 (2016). arXiv:1609.03551 [hep-ph]
74. W. Rodejohann, C.E. Yaguna, JCAP **1512**(12), 032 (2015). arXiv:1509.04036 [hep-ph]
75. A. Biswas, S. Choubey, S. Khan, JHEP **1608**, 114 (2016). arXiv:1604.06566 [hep-ph]
76. R. Ding, Z.-L. Han, L. Huang Y. Liao (in preparation)
77. M. Klasen, F. Lyonnet, F. S. Queiroz, Eur. Phys. J. C **77**(5), 348 (2017). https://doi.org/10.1140/epjc/s10052-017-4904-8. arXiv:1607.06468 [hep-ph]
78. K. Dick, M. Lindner, M. Ratz, D. Wright, Phys. Rev. Lett. **84**, 4039 (2000). arXiv:hep-ph/9907562
79. H. Murayama, A. Pierce, Phys. Rev. Lett. **89**, 271601 (2002). arXiv:hep-ph/0206177
80. D.G. Cerdeno, A. Dedes, T.E.J. Underwood, JHEP **0609**, 067 (2006). arXiv:hep-ph/0607157
81. S. Heinemeyer et al. [LHC Higgs Cross Section Working Group]. arXiv:1307.1347 [hep-ph]
82. G. Aad et al. [ATLAS and CMS Collaborations], JHEP **1608**, 045 (2016). arXiv:1606.02266 [hep-ex]
83. H. Baer et al.. arXiv:1306.6352 [hep-ph]
84. G. Aad et al. [ATLAS Collaboration], JHEP **1404**, 169 (2014). arXiv:1402.7029 [hep-ex]
85. V. Khachatryan et al. [CMS Collaboration], Eur. Phys. J. C **74**(9), 3036 (2014) arXiv:1405.7570 [hep-ex]
86. G. Cacciapaglia, C. Csaki, G. Marandella, A. Strumia, Phys. Rev. D **74**, 033011 (2006). arXiv:hep-ph/0604111
87. G. Aad et al. [ATLAS Collaboration], Phys. Rev. D **90**(5), 052005 (2014). arXiv:1405.4123 [hep-ex]. The ATLAS collaboration [ATLAS Collaboration], ATLAS-CONF-2016-045, ATLAS-CONF-2017-027
88. N. Okada, S. Okada, Phys. Rev. D **93**(7), 075003 (2016). arXiv:1601.07526 [hep-ph]
89. L. Basso, A. Belyaev, S. Moretti, C.H. Shepherd-Themistocleous, Phys. Rev. D **80**, 055030 (2009). arXiv:0812.4313 [hep-ph]